Magnetic Properties of Nanostructured CoPt and FePt Thin Films

Sangki Jeong, Yu-Nu Hsu, David E. Laughlin, and Michael E. McHenry

Abstract—Polycrystalline MgO underlayer films lead to different preferred orientations of $L1_0$ CoPt and FePt films after the annealing process, depending on the thickness of $L1_0$ films. $L1_0$ films with a thickness greater than 20 nm revealed mostly $L1_0$ [100] fiber texture and consequently in-plane anisotropy as determined by magnetic hysteresis. Strong perpendicular anisotropy due to the $L1_0$ [001] fiber texture was obtained for thicknesses below 10 nm. The δM curve showed strong intergranular exchange coupling. The angular variation of coercivity showed the possibility of both domain wall motion and a rotational mechanism of magnetization reversal.

Index Terms—CoPt, FePt, in-plane anisotropy, perpendicular anisotropy, recording media, thin films.

I. INTRODUCTION

ORDERED $L1_0$ CoPt and FePt thin films have large anisotropy constants and have received attention for their potential application for extremely high density recording [1]. The feasibility of the use of these materials will be increased if control of the easy axis—either in-plane or perpendicular directions—can be obtained. Fine grains and magnetization reversal by rotation will aid in obtaining an acceptable signal to noise ratio [2], [3]. In this paper, the possibility of controlling the easy axis orientation will be investigated and the details of the magnetic properties and the possible reversal mechanisms in polycrystalline thin films will be discussed based on the magnetic properties and microstructure.

II. EXPERIMENTAL PROCEDURE

All films were prepared by RF diode sputtering on (100) oxidized Si substrates under 3–10 mtorr of Ar gas. An alloy target of CoPt, a MgO target and Pt chips on a Fe target were used to synthesize the magnetic and underlayer films. The samples were annealed in a rapid thermal annealer under an Ar atmosphere. Magnetic properties were measured using Vibrating Sample Magnetometry (VSM), Alternating Gradient Force Magnetometry (AGFM), and SQUID Magnetometry, with maximum fields of 14–50 kOe. Structural and microstructural properties were examined by X-ray diffractometry (Cu-Kα, 35 kV, 20–25 mA) and transmission electron microscopy (TEM).

TABLE I
THE SAMPLE REPRESENTATIONS

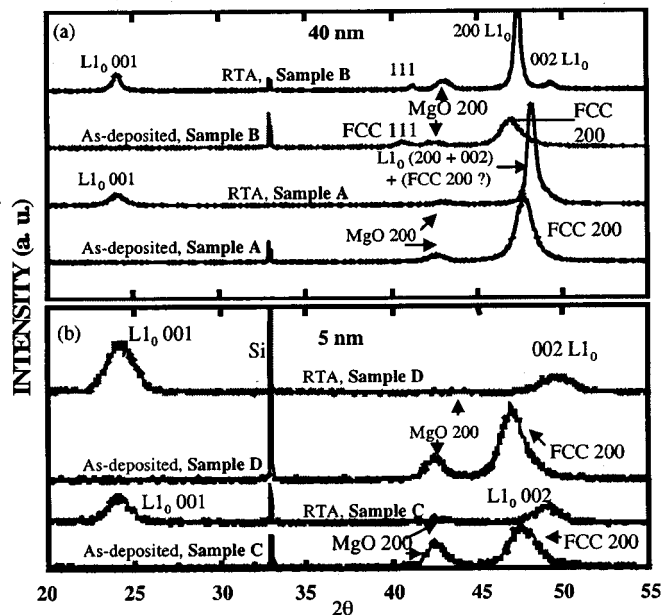| Sample	Film structure
A	CoPt 40 nm/MgO 10 nm/Oxidized Si
B	FePt 40 nm/MgO 10 nm/Oxidized Si
C	SiO_2/CoPt 5 nm/MgO 10 nm/Oxidized Si
D	SiO_2/FePt 5 nm/MgO 10 nm/Oxidized Si

Fig. 1. X-ray $\theta/2\theta$ diffraction spectra of (a) the sample A and B before and after the Rapid Thermal Annealing (RTA) at 700°C for 18 minutes(min). (b) the sample C and D before and after RTA at 700°C for 10 minutes.

III. RESULTS AND DISCUSSION

We have prepared four types of samples on Si substrates by varying the thickness of the magnetic layer while fixing the thickness of the MgO films. Table I shows the film layers for the four samples. The chemical compositions of the films were found to be close to $Co_{46}Pt_{54}$ and $Fe_{55}Pt_{45}$ by an X-ray fluorescence method. A $\langle 100 \rangle$ fiber textured FCC phase can be observed in the as-deposited films as seen in Fig. 1.

After the annealing process, the 40 nm thick films (samples A and B) exhibited a small X-ray diffraction (XRD) intensity of the $L1_0$ (001) and $L1_0$ (002) peaks and a high intensity of $L1_0$ (200) reflections, as shown in Fig. 1(a). This indicates a
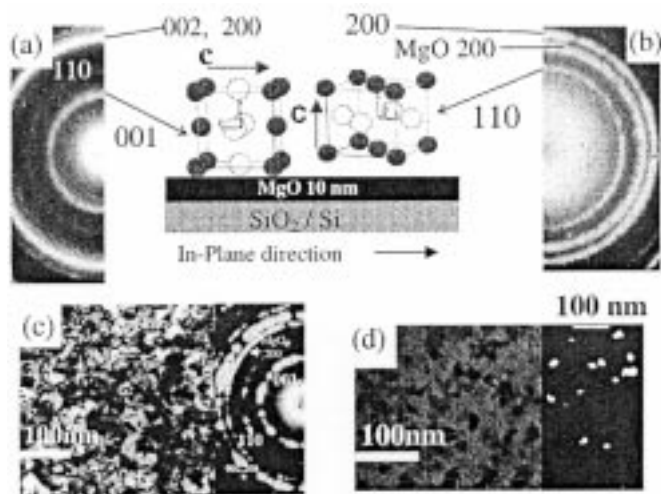
Fig. 2. SAD patterns of (a) the sample A after RTA at 650°C for 8 min. (b) the sample C after RTA at 700°C for 10 min. (c) Bright field image and SAD of the sample A after RTA at 700°C for 18 min. (d) Bright and dark field (200 reflection) images of the sample C after RTA at 700°C for 10 min.

mostly in-plane distribution of the easy axes. There is a possibility that the FCC (200) peak overlaps with $L1_0$ (200) reflection [sample A does not show clear peak splitting of $L1_0$ 200 and 002, Fig. 1(a)], however, the splitting of the $L1_0$ (002) and $L1_0$ (200) peaks for sample B [Fig. 1(a)] supports a $L1_0$ [100] fiber texture. The 5 nm thick films (samples C and D) revealed strong $L1_0$ (001) superlattice-reflections and $L1_0$ (002) reflections, while not showing $L1_0$ (200) reflections [Fig. 1(b)]. Selected area diffraction (SAD) patterns in TEM showed a strong, well separated $L1_0$ (001) reflection and a weak $L1_0$ (110) reflection for sample A [Fig. 2(a)]. However, the 5 nm films (sample C) showed strong $L1_0$ (110) reflections [Fig. 2 (b)].

Based on the I_{001}/I_{110} intensity ratio for sample A in SAD [4] and I_{200}/I_{002} (assuming full ordering) of sample C in XRD, more than 85% of the $L1_0$ c-axes lie in the plane in the 40 nm films. The 5 nm films exhibit all perpendicular variants based on XRD and SAD patterns, although a very weak (001) peak is founded by SAD. Grain size from less than 10 to about 50 nm were observed for the 40 nm films. For the 5 nm films, the grain sizes were found to be less than 30 nm [Fig. 2(c) and (d)]. The 40 nm FePt films (sample B) were found to have randomly oriented grains, based on the (111) XRD reflection and the observation of the (111) ring patterns in SAD.

Fig. 3 shows magnetization curves for CoPt and FePt films after annealing. The 40 nm CoPt films without a MgO underlayer showed [111] fiber texture and similar coercivities (Hc) in the in-plane and perpendicular directions [Fig. 3(a)]. However, due to exchange coupling, those films exhibited higher values of coercive squareness (S^*) and remanence squareness (S), (>0.75 in the in-plane hysteresis).

In-plane anisotropy was inferred from the hysteresis of the highly textured 40 nm CoPt films (sample A) [Fig. 3(b)] with values of S and S^* both over 0.85. The 40 nm FePt films (sample B) exhibited more in-plane anisotropy, than the films without MgO but not as much as CoPt/MgO films (sample A). This is attributed to their degree of texture. On the contrary, the hysteretic response of the 5 nm films (sample C and D) indicates perpen-
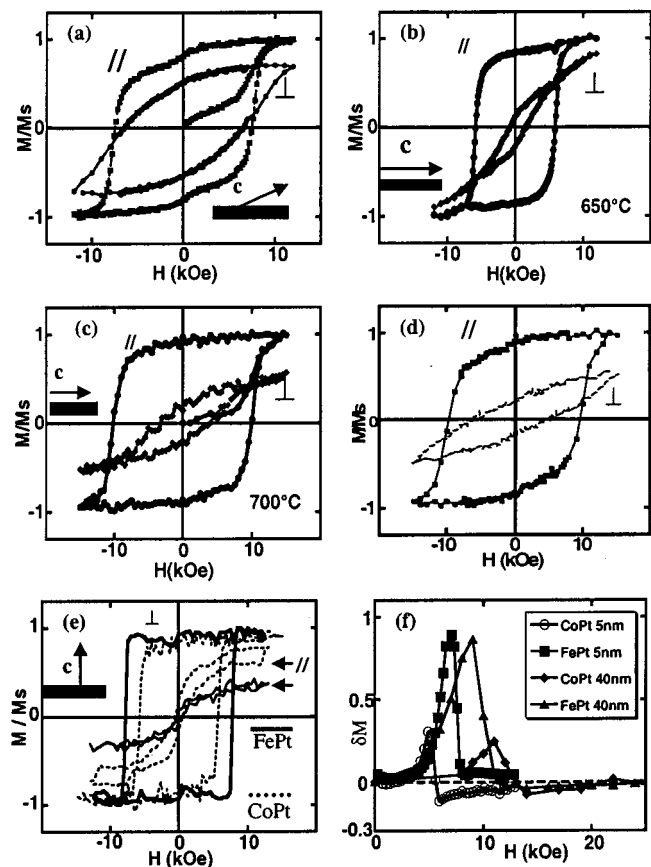

Fig. 3. (a) CoPt 40nm without MgO films, RTA 700°C for 25 min, (111) texture, easy axes of 36° from the plane; (b) Sample A, RTA 650°C for 8 minutes; (c) Sample A, RTA 700°C for 18 minutes; (d) Sample B, RTA 450°C for 10 minutes; (e) sample C and D, RTA 700°C for 10 minutes; (f) δM plots of (c), (d), and (e).

dicular anisotropy [Fig. 3(e)]. Basecd d on the X-ray spectra, coercivities, and using the previously reported [5] relation between coercivity and volume fraction of the ordered phase, the films (Fig. 3) are inferred to be substantially ordered.

The 5 nm films (sample C and D) revealed only one structural variant. Therefore, we can measure the ratio I_{001}/I_{002} in the XRD spectra, which was found to be ~ 1.65 in the CoPt films (sample C), which is close to the calculated value of ~ 1.7. We found it to be ~ 2.5 in FePt films (sample D) which is larger than the calculated value of ~ 1.8. Therefore, these films are inferred to be fully ordered (the structure and Lorentz–Polarization factors were considered in the calculations for the fully ordered $L1_0$ structure).

Magnetic interactions were studied by δM plots and found to indicate strong exchange coupling in most samples [Fig. 3(f)], and the slopes of the M-H loops in Fig. 3(e) exceed $5/(4\pi)$. The critical single domain particle size (Dc) is calculated to be several hundreds of nanometers [3] but was not observed in TEM. However, there is a possibility of incoherent switching during the reversal process for larger grains due to the small exchange length ($l_{ex} = (A/Ms^2)^{1/2} \sim$ 10–20 nm where A is the exchange constant) [4],[6].

Fig. 4(a) shows the angular variation of coercivities of annealed 5 and 40nm films. The theoretical angular variations
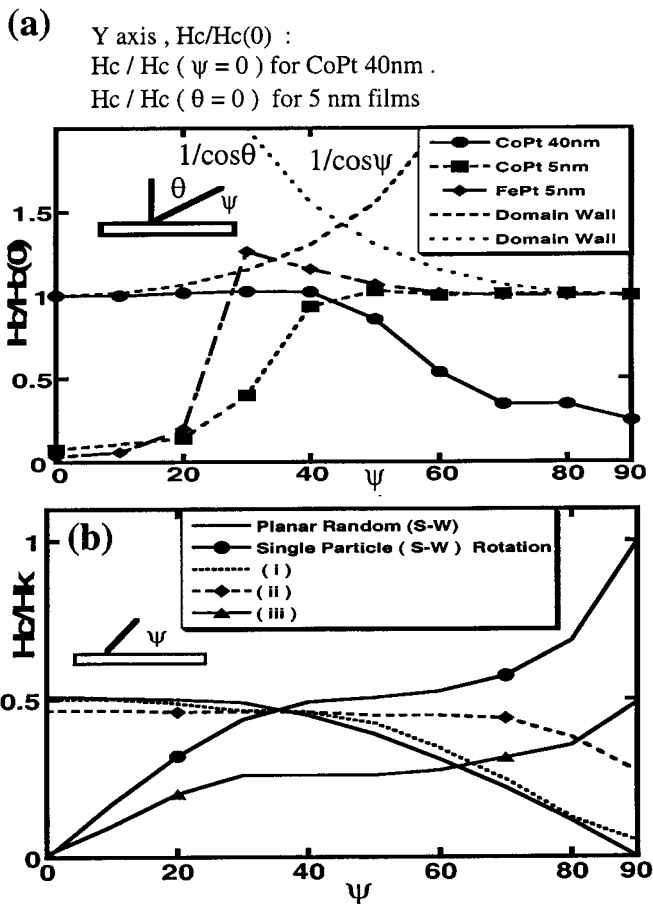
(a) Y axis , Hc/Hc(0) :
Hc / Hc ($\psi = 0$) for CoPt 40nm .
Hc / Hc ($\theta = 0$) for 5 nm films

Fig. 4. (a) Measured angular variations of Hc of Fig. 3(c) and (e). (b) The calculated angular variations of Hc, based on Micromagnetic (MM) calculations of CoPt 5 and 40 nm thick films and Storner–Wohlfarth (S–W). Domain wall motion ($1/\cos\omega$ law) was indicated. α (damping coefficient) = 1 is chosen in all MM calculations. (i) MM calculation of 40 nm films, in-plane 2D distribution of easy axes (Planar Random). (ii) MM calculations for 20% perpendicular variants + Planar Random, same as in (i) but 20% of easy axes are directed out of plane (the perpendicular direction). (iii) MM calculations, easy axes are perpendicular to the films surface.

of the coercivity as predicted by domain wall motion and Stoner–Wohlfarth (S–W) models are indicated in Fig. 4(b). We have simulated the hysteresis of CoPt films using micromagnetic calculations [7], [8]. Calculations use the measured Ms of $\sim$600 emu/cc for CoPt films, an exchange stiffness, A of$\sim 10^{-6}$ erg/cm [3], the measured average grain size (D) of $\sim$20 nm (5 nm CoPt thick films) and $\sim$25 nm (40 nm CoPt films), and assume a value of 10^7 erg/cc for the anisotropy constant (Ku), determined by a rough estimation from the hard axis loop. We consider coherent rotation within each grain. Within this model we have simulated the angular dependence of hysteresis for a planar random distribution of easy axes, with and without a fraction of perpendicular variants [Fig. 4(b)].

The simulation indicated a higher absolute Hc but has a similar angular dependence of coercivities as the experimental data. Since Hc does not follow a $1/\cos\Psi$ dependence or increase at angles corresponding to out of plane directions, it is believed that each particle (in 40 nm films) switches in a coherent rotation mode. The intergranular interaction is relatively weak compared with the anisotropy field Hk ($Ms/Hk < 0.01$). A rough estimate of the Hc/Hk ratio from experimental data is $\sim$0.3, assuming Ku $\sim 10^7$ erg/cc. The exchange coupling constant $C^* = A/KD^2$ used in the simulation can not explain such a small coercivity. The real exchange coupling is apparently much higher. In addition, the remaining FCC phase and the incoherent switching of the larger particles could further lower the Hc. The profiles of angular dependence of Hc in 5 nm films [sample C and D in Fig. 4(a)] were fitted to $1/\cos\theta$ and the deviation from the equation begins to occur at an angle of 20° from the easy axis [Fig. 4(a)]. The simulated angular variation in these films [Fig. 4(b)] also showed much higher Hc and did not show any increased Hc at angles off the easy axis contrary to the experimental data. At higher angles Hc drops rapidly probably due to the rotation mode. Thus, the reversal mechanism seems to occur not only by the domain wall motion but also a rotational mode. The observation of such a small grain size does not support incoherent switching within a grain and multi-domain grains. The intergranular exchange interaction makes it possible to reverse the magnetization by the expansion of a reverse domain through the motion of a domain wall at the lower angles from the perpendicular direction (easy axis) [8]. It is still believed that the spins of a grain rotate coherently for most grains. However, due to the intergranular magnetostatic interactions those grains are not rotating together at higher angles relative to the easy axis [9], [10]. In summary, the reversal mechanism of the 5 nm films does not follow the S–W based theory or micromagnetic calculations that assume coherent rotation within a grain with a intergranular interaction. Further analysis by magnetic viscosity measurements will be required for a more in depth understanding of the reversal mechanism.

REFERENCES

[1] D. J. Sellmyer, M. Yu, and R. D. Kirby, *Nano-98*, June 1998.
[2] T. Suzuki, N. Honda, and K. Ouchi, *J. Appl. Phys.*, vol. 85, p. 4301, 1999.
[3] D. Weller, A. Moser, and L. Folks, *et al.*, *TMRC 99*.
[4] S. Jeong, Y.-N. Hsu, D. E. Laughlin, and M. E. McHenry, *44th Annual Conference, MMM 99*.
[5] R. A. Ristau, Ph.D. dissertation, Lehigh Univ., 1998.
[6] Y. Chen, Ph.D. dissertation, Carnegie Mellon Univ., 1998.
[7] P.-L. Lu, Ph.D. dissertation, Carnegie Mellon Univ., 1995.
[8] J. G. Zhu, Ph.D. dissertation, Univ. of California (UCSD), 1989.
[9] L. Zhang and A. Manthiram, *Phys. Rev.*, vol. 54, p. 3462, 1996.
[10] ——, *Phys. Rev.*, vol. 517, p. 319, 1998.